Conformational Distributions of Protease−Serpin Complexes: A Partially Translocated Complex†

Lu Liu,‡ Nicole Mushero,§ Lizbeth Hedstrom,|| and Anne Gershenson*,‡

Department of Chemistry, Graduate Program in Biochemistry, and Department of Biochemistry, Brandeis University, 415 South Street, Waltham, Massachusetts 02454

Received May 14, 2006; Revised Manuscript Received July 8, 2006

ABSTRACT: Serpins regulate serine proteases by forming metastable covalent complexes with their targets. The protease docks with the serpin and cleaves the serpin's reactive center loop (RCL) forming an acylenzyme intermediate. Cleavage triggers insertion of the RCL into β sheet A, translocating the attached protease ~70 Å and disrupting the protease active site, trapping the acylenzyme intermediate. Using single-pair Förster resonance energy transfer (spFRET), we have measured the conformational distributions of trypsin and α_1-proteinase inhibitor (α_1PI) covalent complexes. Bovine trypsin (BTryp) complexes display a single set of conformations consistent with the full translocation of BTryp ($E_{full}I^*$). However, the range of spFRET efficiencies is large, suggesting that the region around the trypsin label is mobile. Most complexes between α_1PI variants and the more stable rat trypsin (RTryp) also show a single set of conformations, but the conformational distribution is narrower, indicating less disruption of RTryp. Surprisingly, RTryp complexes containing α_1PI labeled at Cys232 with a cationic fluorophore display two equally populated conformations, $E_{full}I^*$ and a conformation in which RTryp is only partially translocated ($E_{part}I^*$). Destabilizing the RTryp active site, by substituting Ala for Ile16, increases the $E_{full}I^*$ population. Thus, interactions between anionic RTryp and cationic dyes likely exert a restraining force on α_1PI, increasing the energy needed to translocate trypsin, and this force can be counteracted by active site destabilization. These results highlight the role of protease stability in determining the conformational distributions of protease−serpin covalent complexes and show that full translocation is not required for the formation of metastable complexes.

Inhibitory members of the serpin superfamily are involved in a variety of intricately regulated physiological processes, including inflammation and blood coagulation (*1*, *2*). Unlike canonical protease inhibitors that simply block the protease active site, serpins form a stable, covalent adduct with their target proteases. The first steps in covalent complex formation are the same as substrate hydrolysis: (A) docking of the protease E with the serpin I to form an encounter complex E·I and (B) cleavage of the serpin's reactive center loop RCL[1] and formation of the acylenzyme intermediate E−I, containing a covalent bond between the cleaved RCL and the catalytic Ser195 (Figure 1, scheme 1). Like substrate acylenzymes, E−I can hydrolyze, releasing the protease and the cleaved serpin (I*) in which the RCL has inserted into β sheet A. Alternatively, the RCL can insert into β sheet A while the acylenzyme is still intact, translocating the attached protease as much as 70 Å across the serpin and disabling the active site (Figure 1). The resulting covalent complex E−I* circulates for hours *in vivo* before being internalized, but it is stable for days *in vitro* (*2*, *3*). The covalent linkage between the protease and serpin eventually hydrolyzes, releasing active protease and I*. Although maximal disruption of the protease structure is thought to occur during the final steps in translocation (*4*), how translocation and inactivation are coupled is not understood. Both the force from pulling on the catalytic Ser and contact between the protease and serpin are likely to distort the protease structure.

The conformation and conformational distributions of E−I* complexes are still a matter of some dispute despite the determination of the X-ray crystal structures for two covalent complexes containing the serpin α_1-proteinase inhibitor (α_1PI, also known as α_1-antitrypsin) (*5*, *6*). In both the bovine trypsin (BTryp)−α_1PI and porcine pancreatic elastase (PPE)−α_1PI complexes, the protease is fully translocated, and the catalytic Ser195 is pulled >3 Å out of the active site (*5*, *6*). This perturbation is sufficient to disable the catalytic triad and stabilize the acylenzyme intermediate. However, although the structure of PPE is largely intact (*6*), 37% of the BTryp tertiary structure is missing, presumably because of structural mobility (*5*). In addition, the orientation of the two proteases relative to α_1PI is quite different such that residues that align within 2 Å for the free protease

† This work was funded by NSF Grant MCB-0446220, and N.M. was supported by NIH Grant GM07956.

* To whom correspondence should be addressed. Phone: 781-736-2548. Fax: 781-736-2516. E-mail: gershenson@brandeis.edu.

‡ Department of Chemistry.

§ Graduate Program in Biochemistry.

|| Department of Biochemistry.

[1] Abbreviations: BTryp, bovine trypsin; FRET, Förster resonance energy transfer; α_1PI, human α_1-proteinase inhibitor; PPE, porcine pancreatic elastase; RCL, reactive center loop; RTryp, rat anionic trypsin; SI, stoichiometry of inhibition; spFRET, single-pair Förster resonance energy transfer.

10.1021/bi0609568 CCC: $33.50
Published on Web 08/16/2006

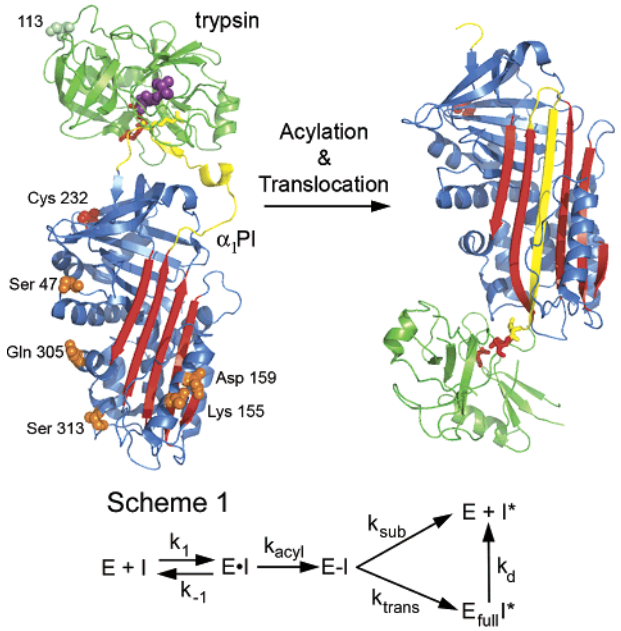

FIGURE 1: Protease inactivation by serpins. The protease, E, and serpin, I, dock to form the encounter complex, E·I, shown on the left ((*30*), pdb:1oph). The RCL is then cleaved, resulting in the acylenzyme intermediate, E−I, which partitions between a substrate-like pathway yielding *E* and *I**, and the inhibitory pathway where the RCL also inserts into β sheet A and the attached protease is translocated, forming $E_{full}I^*$, shown on the right ((*5*), pdb:1ezx). The protease, BTryp, is green with the catalytic triad in red. The Ile16−Asp194 salt bridge is purple, and the location of the donor fluorophore is in green spacefill. The serpin, α_1PI, is shown in blue with the RCL in yellow, β sheet A in red, Cys 232 in crimson spacefill, and single Cys mutations in orange. Protein figures were made using PYMOL (Delano Scientific). The generally accepted scheme for protease−serpin covalent complex formation is shown at the bottom.

structures can be >10 Å apart when the covalent complex structures are aligned. NMR studies of the BTryp−α_1PI complex also show a single fully translocated conformation (*7*), but multiple conformations, including a partially translocated structure, are observed in time-resolved ensemble Förster resonance energy transfer (FRET) studies of rat anionic trypsin−α_1PI (RTryp−α_1PI) (*8*). Kinetic experiments also fail to reach a consensus. Although some protease−serpin complexes display only a single reactivation rate constant (*9*), other complexes have multiple reactivation rate constants suggesting that at least two conformations are present (*9*, *10*). Many explanations have been put forth to explain these contradictions, including differences in conformational distributions between specific protease−serpin pairs, fluorescence artifacts, and proteolytic degradation of the complexes.

We report here on the use of single-pair Förster resonance energy transfer (spFRET) to probe the conformational heterogeneity of α_1PI covalent complexes with BTryp and RTryp. The conformational distributions of BTryp−α_1PI complexes are generally wider than those observed for RTryp complexes, indicating greater disruption of the BTryp structure. In addition, we have trapped a partially translocated conformation for RTryp but not BTryp covalent complexes. The increased stability of the RTryp active site as well as interactions between anionic RTryp and cationic dyes accounts for the failure to observe this conformation in BTryp complexes.

EXPERIMENTAL PROCEDURES

Trypsin Preparation. Chymotrypsinogen amino acid numbering is used for all trypsin variants. The K113C RTryp variant has previously been characterized; α_1PI inhibits K113C RTryp at a 1:1 stoichiometry, and the observed rate constant for inhibition is comparable to that for wild-yype RTryp (*8*). The K113C/I16A rat anionic trypsinogen II variant was generated using Quikchange (Stratagene). Rat anionic trypsinogen II variants were expressed in *Saccharomyces cerevisiae* strain DLM101α, purified, and activated as previously described (*11*, *12*). The bTrygen/pQE60 plasmid containing the coding sequence for bovine cationic trypsinogen was the generous gift of Peter Gettins (University of Illinois). The S113C mutation was introduced using Quikchange. Bovine trypsinogen was expressed as inclusion bodies in *Escherichia coli* strain SG13009, refolded, purified, and activated as previously described (*13*).

α_1PI Preparation. The pEAT8−137 plasmids containing the coding sequence for wildtype α_1PI and the Cys232Ser (C232S) α_1PI variant were the generous gift of Charles L. Cooney (MIT). The pEAT8 sequence contains two natural sequence variations, a His to Arg mutation at residue 101 and a Glu to Asp mutation at 376, which do not affect function (*14*). The following single Cys mutations were introduced into the C232S background S47C, K155C, D159C, Q305C, and S313C. All α_1PI variants were expressed as inclusion bodies in *E. coli* BL21(DE3) cells, refolded, and purified using a variation of previously published methods (*15*−*17*). Inclusion bodies were solubilized at 4 °C overnight in 8 M urea, 50 mM Tris-HCl, pH 8.0, 1 mM EDTA, and 1 mM DTT. The unfolded protein was subsequently diluted 10-fold into 10 mM Tris-HCl, pH 8.0, 10 mM NaCl, and 0.1 mM DTT and dialyzed overnight. The refolded protein was then applied to a HiTrap Q Fastflow Sepharose ion exchange column (GE Healthcare) and eluted at 200 mM NaCl in the Tris-HCl (pH 8.0) buffer. Fractions containing α_1PI were identified by SDS−PAGE, pooled, and dialyzed overnight into 10 mM Bis-Tris, pH 6.3, 10 mM NaCl, and 0.1 mM DTT. The protein was applied to a Source 15Q PE ion exchange column (GE Healthcare) and eluted at 60 mM NaCl in the Bis-Tris (pH 6.3) buffer.

Stoichiometry of Inhibition (SI). Trypsin variants were titrated with *p*-nitrophenyl-*p*′-guanidinobenzoate HCl (Sigma Chemical) to determine the concentration of active enzyme (*18*). Greater than 90% of the trypsin was active both before and after dye labeling. The SI, the ratio of moles of serpin needed to inactivate one mole of active trypsin, was determined by titrating trypsin with α_1PI as previously described (*19*). SIs were 1 for labeled and unlabeled trypsin and α_1PI.

Protein Labeling. Trypsin variants were labeled at residue 113 with Alexa Fluor 555 maleimide (Invitrogen), Atto 610 maleimide (Atto-Tec), or Alexa Fluor 488 maleimide (Invitrogen) according to the manufacturer's instructions. Free dye was separated from trypsin using a soybean trypsin inhibitor column (Sigma Chemical). Wild-type α_1PI and single Cys variants were labeled with Cy5 maleimide (GE Healthcare), Atto 610 maleimide or Texas Red maleimide (Invitrogen) according to the manufacturer's instructions. A PD-10 gel filtration column (GE Healthcare) was used to

separate α_1PI from the free dye. The labeling efficiencies were 0.1 to 0.3 for trypsin and 0.5 to 0.8 for α_1PI.

R_o, the distance between donor and acceptor at which there is 50% energy transfer, was calculated as 59 Å for both Alexa Fluor 555−Cy5 and Alexa Fluor 555−Atto 610 and as 48 Å for Alexa Fluor 488−Texas Red using (*20*)

$$R_o = 9.78 \times 10^3(\kappa^2 n^{-4} Q_D J(\lambda))^{1/6} \quad (1)$$

where the relative orientation of the dipoles was assumed to be randomized, resulting in an orientation factor, κ^2, of 2/3. The refractive index, n, was assumed to be 1.33. Q_D is the quantum yield of the donor, and $J(\lambda)$ is the overlap integral of the donor emission spectrum with the acceptor absorption spectrum. Quantum yields of 0.4 and 0.7 were used for Alexa Fluor 488 and Alexa Fluor 555, respectively. Overlap integrals were calculated using the donor emission and acceptor absorption spectra of singly labeled complexes.

spFRET Data Collection and Analysis. Donor-labeled trypsin variants (0.5 to 2 μM) were mixed at a ratio of 1:2 with acceptor-labeled α_1PI in 50 mM HEPES, pH 7.4, and 100 mM NaCl. After 15 min, the samples were diluted to 50−100 pM in the presence of 10 mM of benzamidine to prevent proteolysis by free trypsin. The fluorescence of single complexes was collected using a one photon single molecule confocal setup with a 100 μm pinhole based on an IX-70 inverted microscope (Olympus) (*21*) (Figure S1, Supporting Information). The excitation wavelengths, from an air-cooled argon−krypton laser (Melles-Griot) were 520 and 488 nm for covalent complexes labeled with Alexa Fluor 555 and Alexa Fluor 488, respectively. After being split by color, fluorescence was detected by two single photon counting avalanche photodiodes (APDs, Perkin-Elmer, SPCM-AQR-14) and collected at 24 MHz using a two-channel data acquisition card and associated software (ISS). A detailed description of the optical setup is provided in Supporting Information.

Data from the donor and acceptor channels were binned at 1 kHz and a threshold of 40 total, acceptor plus donor, photon counts was used to identify photon bursts arising from complexes diffusing through the focal volume. The photon counts were corrected for background fluorescence and for leakage of donor fluorescence into the acceptor channel. The spFRET efficiency, E, was calculated using (*21*)

$$E = \frac{I_A}{(I_D + \gamma I_A)} \quad (2)$$

$$\gamma = \frac{\phi_A \eta_A}{\phi_D \eta_D} \quad (3)$$

where I is the corrected photon count, and D and A denote the donor and acceptor channels, respectively. The γ factor corrects for differences in the probability of detecting a photon from the donor or acceptor because of differences in the quantum yield, ϕ, or the detection efficiency of the APDs in different regions of the spectrum, η. For singly labeled samples with identical optical densities at the excitation wavelength, 520 nm, γ is the ratio of the fluorescence intensity of the acceptor-only samples to that of the donor-only samples measured on the single molecule fluorescence setup (*22*). γ factors were measured using labeled trypsin and labeled α_1PI as well as singly labeled trypsin−α_1PI covalent complexes. In general, $\gamma = 1$, with the exception of RTryp−α_1PI complexes labeled with Atto 610 at position 232. For these complexes, $\gamma = 2$. The change in γ arises from an increase in Atto 610 fluorescence intensity. Although the value of γ alters the location of the peaks in the spFRET histograms, the number of peaks remains constant.

SpFRET histograms were generated in Matlab (Mathworks) using efficiencies calculated according to eq 2. Histograms were analyzed using Matlab and Origin (Originlab). The spFRET histogram peak areas, half-widths, and maxima were determined using Gaussian fits to the data.

Fluorescence Anisotropy. Steady state, ensemble fluorescence polarization experiments were conducted on a Fluorolog fluorometer (ISA). Single molecule polarization experiments were conducted by replacing the dichroic filter used to separate donor and acceptor fluorescence with a polarizing beam splitter (Newport). Samples were excited at 520 nm for Alexa Fluor 555 and 568 nm for Atto 610 (Supporting Information).

RESULTS

Characterization of Dye Labeled Proteins and Experimental Design. Trypsins were labeled with the donor dye at a single Cys engineered at position 113 (Ser in BTryp and Lys in RTryp), and α_1PI was labeled with the acceptor dye on either the native Cys232 or at single Cys mutations introduced into the C232S background (Figure 1). In the X-ray crystal structure of the BTryp−α_1PI covalent complex, more than 30% of the trypsin structure, including the loop containing residue 113, is disordered (*5*). Therefore, distances between the trypsin and α_1PI labels were estimated by aligning free BTryp (*23*) with the BTryp−α_1PI covalent complex structure using Swiss-Pdb Viewer (*24*). The selected donor−acceptor pairs Alexa Fluor 555−Atto 610 and Alexa Fluor 555−Cy5 have R_o values equal to 59 Å, resulting in significant FRET efficiencies over the entire anticipated range of distances, 30−90 Å.

The labeled proteins were active with a stoichiometry of inhibition of ~1 for all protein samples. Covalent complexes were formed by mixing trypsin and α_1PI at a ratio of 1:2 for 15 min, and their presence was confirmed by SDS−PAGE (data not shown). Although the high concentrations and prolonged incubation times for X-ray crystallography and NMR spectroscopy may permit degradation of the complexes by reactivated trypsin, autoproteolysis is avoided in the spFRET experiments by the low concentrations of complexes (50−100 pM), comparatively rapid data acquisition, and by the presence of the trypsin inhibitor benzamidine (10 mM). The spFRET of diffusing covalent complexes was measured using a confocal fluorescence microscope to limit the observation volume (Figure S1, Supporting Information). Under these conditions, the average number of complexes in the observation volume is less than one. When a complex diffuses through the observation volume, a burst of donor and/or acceptor fluorescence is observed (Figure 2A). The spFRET efficiencies are calculated for each burst, using eq 2, as described in Experimental Procedures, and these efficiencies are displayed in histograms (Figure 2).

Bovine Trypsin−α_1PI Covalent Complexes Have a Wide Conformational Distribution. The spFRET histograms for

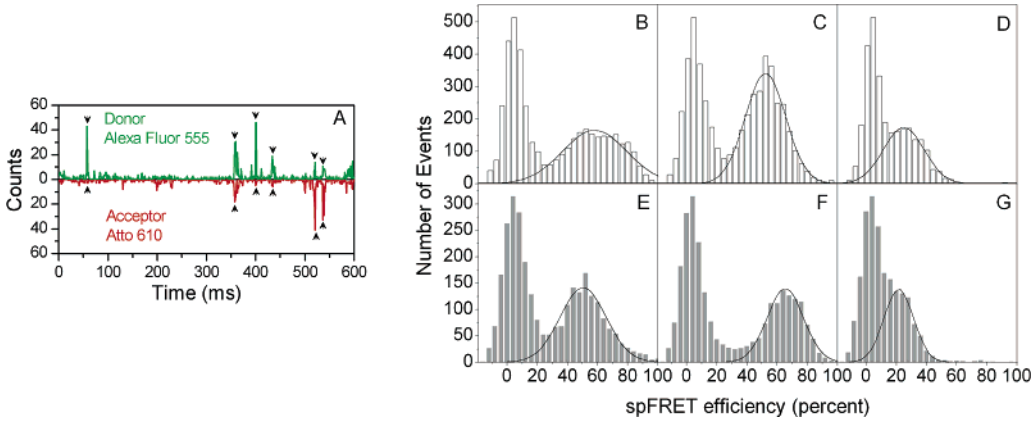

FIGURE 2: SpFRET experimental results for trypsin−α_1PI covalent complexes in 50 mM HEPES, pH 7.4, 100 mM NaCl, and 10 mM benzamidine. Trypsin is labeled with Alexa Fluor 555 (donor) at position 113, and α_1PI is labeled with the acceptor dye at the position denoted in parentheses. (A) Sample data, binned at 1 kHz, for labeled RTryp−α_1PI covalent complexes, where the arrows indicate signals from single complexes diffusing through the excitation volume. (B−D) Histograms for BTryp complexes. (E−G) Histograms for RTryp complexes. (B and E) Atto 610−α_1PI(47); (C and F) Atto 610−α_1PI(159); (D and G) Cy5−α_1PI(232).

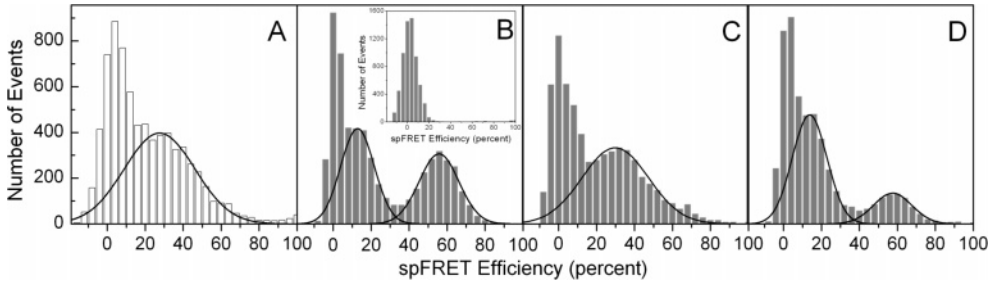

FIGURE 3: SpFRET histograms of RTryp complexes showing a partially translocated conformation. (A) Alexa Fluor 555−BTryp and Atto 610−α_1PI(232). (B) Alexa Fluor 555−RTryp and Atto 610−α_1PI(232). The inset shows the spFRET histogram for Alexa Fluor 555−RTryp containing the S195A mutation, which can only form the encounter complex, E·I, and Atto 610−α_1PI. (C) Alexa Fluor 488−RTryp and Texas Red−α_1PI(232). (D) Alexa Fluor 555−RTryp containing the destabilizing I16A mutation and Atto 610−α_1PI(232).

all BTryp covalent complexes display two peaks (Figures 2 and 3, Table 1). The first peak, centered at 0% energy transfer, results from complexes containing only the donor dye as well as complexes in which the acceptor dye has photobleached. Because the actual background at any time can be more or less than the average background, the corrected fluorescence intensity may be negative leading to the negative spFRET efficiencies seen in the tail of this zero peak. The second peak reports on the conformations of diffusing covalent complexes. The center of the second peak varies with Atto 610 and Cy5 as well as with the location of the α_1PI label. In all cases, the efficiencies are consistent with the full translocation of trypsin relative to α_1PI, as observed in the crystal structure (hereafter termed $E_{full}I^*$) (Table 1) (*5*, *6*). All of the $E_{full}I^*$ peaks have half-widths greater than 10% (Table 1), indicating variations in the distance between donor and acceptor dyes. This variation is further increased when α_1PI is labeled at position 47, which is located in a mobile loop (Figure 1). The consistent, unexpectedly large widths of the $E_{full}I^*$ peaks suggest that the tertiary structure of BTryp is mobile in the vicinity of 113, in agreement with the BTryp crystal structure.

Rat Trypsin−α_1PI Covalent Complexes Have a Narrow Conformational Distribution. The spFRET histograms for most covalent complexes between RTryp and α_1PI show two peaks similar to those observed for BTryp complexes (Figure 2, Table 1). However, the peak centers are shifted to significantly higher efficiencies when the acceptor is located at positions 155 and 159 and to lower efficiencies when the acceptor is at position 305. The sequences of BTryp and RTryp are 73% identical, and all of the Trp residues and disulfide bonds, which are known to quench fluorophores, are conserved. In addition, modeling RTryp (*25*) into the BTryp−α_1PI covalent complex structure (*5*) does not change the estimated distances between the dyes. Thus, these effects will not explain the differences between the BTryp and RTryp complexes.

As with the BTryp complexes, the spFRET efficiencies for the RTryp covalent complexes are consistent with full translocation. However, the differences in mean spFRET efficiency suggest that the orientation of trypsin relative to α_1PI is not the same in the RTryp and BTryp complexes. Perhaps the RTryp complex resembles that for PPE (*6*). In addition, the spFRET peaks for RTryp are consistently narrower than those for the corresponding BTryp complexes (Figure 2, Table 1), suggesting that RTryp is less structurally disrupted.

Covalent Complex Dissociation. Greater structural disruption of BTryp in covalent complexes could result in more stable complexes. Therefore, changes in the spFRET histograms were used to monitor covalent complex dissociation. For BTryp complexes, the area of the $E_{full}I^*$ peak decreased exponentially with time yielding an apparent dissociation rate constant of $(6.1 \pm 0.3) \times 10^{-6}$ s^{-1}, in good agreement with the literature values (*9*). The dissociation rate constant for RTryp complexes is $(7.8 \pm 0.4) \times 10^{-6}$ s^{-1}, similar to that for BTryp. Thus, as observed for BTryp−α_1PI complexes and the more intact PPE−α_1PI complexes (*6*), differences

Table 1: SpFRET Peak Centers and Half-widths for the Non-zero Peaks[a]

location of the label in α_1PI	bovine trypsin peak center (%)	bovine trypsin peak half-width (%)	rat trypsin peak center (%)	rat trypsin peak half-width (%)
47	55 ± 2	21 ± 2	50 ± 2	15 ± 2
155	65 ± 1	14 ± 1	76 ± 1	10 ± 1
159	52 ± 1	14 ± 1	66 ± 1	11 ± 1
305	77 ± 2	15 ± 3	68 ± 2	10 ± 1
313	78 ± 1	13 ± 2	74 ± 1	10 ± 1
232	27 ± 3	17 ± 2	14 ± 2 ($E_{part}I^*$): 58 ± 1	9 ± 2 10 ± 2
232 (Cy5)	22 ± 1	15 ± 2	20 ± 2	12 ± 2
232 (Texas Red) trypsin (Alexa Fluor 488)	N.M.	N.M.	O.Z. ($E_{part}I^*$): 31 ± 1	O.Z. 16 ± 2
232 (Alexa Fluor 555) trypsin (Atto 610)	N.M.	N.M.	21 ± 1	10 ± 1
232 I16A trypsin	N.M.	N.M.	14 ± 2 ($E_{part}I^*$): 57 ± 1	9 ± 2 11 ± 2

[a] Except as noted, α_1PI is labeled with Atto 610, and trypsin is labeled with Alexa Fluor 555. α_1PI is labeled on single Cys residues located at the listed positions. Cys232 is the native Cys; all other α_1PI variants contain a Ser substitution at this position and Cys substitutions at S47, K155, D159, Q305, or S313. Trypsins are labeled on a single Cys engineered at position 113 (S113 in BTryp and K113 in RTryp). Peak centers and half-widths were determined from Gaussian fits to the data. The uncertainties are the standard deviations of the fits to at least three independent datasets. N.M. = not measured, O.Z.= obscured by the zero peak in the spFRET histograms.

in protease structural disruption have no significant effect on complex dissociation.

Observation of a New Conformation. Surprisingly, spFRET histograms display three peaks when Alexa Fluor 555 labeled RTryp forms a covalent complex with α_1PI labeled with Atto 610 at position 232 (Figure 3B): the 0% peak, a 14% peak consistent with $E_{full}I^*$, and a third peak at 58% efficiency, which corresponds to a conformation in which the donor and acceptor dyes are closer together than is possible in $E_{full}I^*$. The 14% and 58% peaks have approximately equal areas, indicating that both conformations are equally populated. To further confirm the presence of a new conformation, RTryp and α_1PI were labeled with Alexa Fluor 488 (donor) and Texas Red (acceptor), respectively. The value of R_o is 48 Å for this dye pair, which would result in negligible energy transfer when RTryp is fully translocated. Nonetheless, the spFRET histogram displays two peaks, the first at 0% and the second centered at 31% (Figure 3C), confirming the presence of a new conformation ($E_{part}I^*$).

Because of incomplete averaging over dye orientations as well as possible quenching by amino acids such as Trp, the distances determined from spFRET data are only approximations. For the $E_{part}I^*$ peak, the approximate distance between the dyes is 55 Å for both dye pairs, indicating that RTryp is only partially translocated. In addition, the apparent dissociation rate constant of $E_{part}I^*$ is $(1.3\pm0.2) \times 10^{-4}$ s^{-1}, 2 orders of magnitude larger than that for the $E_{full}I^*$ peak, which is also consistent with only partial translocation of RTryp. The appearance of $E_{part}I^*$ is also in qualitative agreement with the time-resolved ensemble FRET experiments on RTryp−α_1PI complexes using fluorescein-labeled RTryp and tetramethylrhodamine-labeled α_1PI (232) (*8*). However, no additional peak is observed when α_1PI is labeled with Cy5 at position 232, when the dyes are reversed (Atto 610-labeled RTryp and Alexa Fluor 555-labeled α_1-PI(232)), or when α_1PI is labeled at other positions as noted above. These observations suggest that the second conformation results from specific dye interactions with RTryp.

Reassessing R_o for RTryp Complexes with Cationic Dyes. Interestingly, Atto 610, Texas Red, and tetramethylrhodamine are all positively charged, which may facilitate interactions with the anionic rat trypsin, whereas Cy5 and Alexa Fluor 555, which do not populate $E_{part}I^*$, both contain a negative charge. Therefore, the additional peak might arise from interactions between the dye and protease, which would be different for cationic BTryp and anionic RTryp. Such interactions could alter R_o, leading to an apparent change in spFRET efficiency. To alter R_o, RTryp−dye interactions would have to change the overlap between the donor emission and acceptor absorption spectra, $J(\lambda)$, the distribution of donor quantum yields, Q_D, and/or relative orientations of the donor and acceptor, κ^2 (see eq 1). We performed several experiments to address these possibilities.

We measured the emission spectra of complexes containing only donor-labeled RTryp or only acceptor-labeled α_1-PI. Although a 4 nm red shift is observed in the Atto 610 (acceptor) absorption spectrum, the peak also broadens, and no significant changes are observed in $J(\lambda)$ or R_o. We also measured the relative quantum yields for all singly labeled covalent complexes. There are no significant differences in measured Alexa Fluor 555 (donor) intensities. The quantum yield of Atto 610 almost doubles in the covalent complexes, but this increase does not affect R_o. To correct for the change in quantum yield, a γ value of 2 is used to calculate the spFRET efficiencies (eqs 2 and 3). Using a γ of 1 shifts the peaks to higher efficiencies but does not alter the number of peaks in the spFRET histograms.

As is usual when calculating R_o, the relative orientations of the donor and acceptor dipoles were assumed to be randomized, resulting in a κ^2 value of 2/3 (eq 1). However, although the orientations will be randomized over an ensemble of complexes, single complexes diffuse through the focused laser spot too quickly for randomization to occur, and the assumption that $\kappa^2 = 2/3$ may not be valid (*26*). This orientation problem is, however, not unique to particular RTryp complexes and, therefore, seems unlikely to account for differences between dyes. Nevertheless, we measured the ensemble steady state anisotropy of singly labeled BTryp and RTryp complexes. Single molecule polarization experiments were also performed for these proteins (Figure S2, Supporting Information). No significant difference was found between anisotropies for the free proteins and complexes, nor were differences observed between BTryp and RTryp complexes (Table 2). There were also no significant differences in the single molecule polarization histograms (Figure S2, Supporting Information).

Looking for the Encounter Complex. The dyes are quite large, and when attached to Cys232, can approach within 2−4 Å of the trypsin surface in the encounter complex, E·I, where the protease and serpin have docked, but no cleavage has occurred (scheme 1, Figure 1). Thus, dye−RTryp

Table 2: Ensemble Steady State Fluorescence Anisotropies, r^a

sample	r
Alexa Fluor 555 RTryp	0.26
Alexa Fluor 555 RTryp−α_1PI	0.25
Atto 610 α_1PI	0.18
RTryp-Atto 610 α_1PI	0.18

[a] RTryp is labeled at position 113, and α_1PI is labeled at position 232.

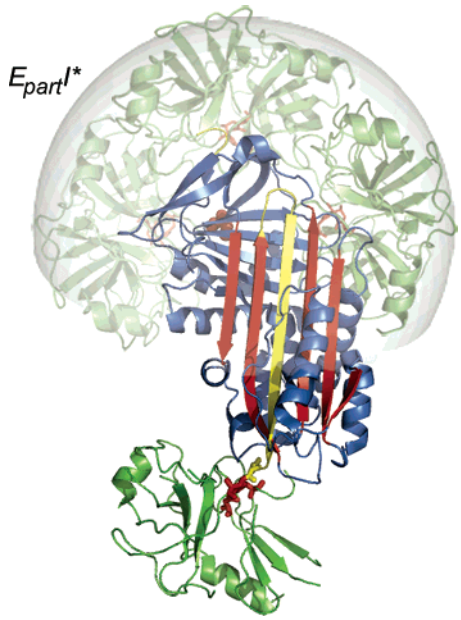

FIGURE 4: Possible locations of RTryp, shaded area, in the $E_{part}I^*$ species superimposed on the X-ray crystal structure of BTryp $E_{full}I^*$ (*5*). Trypsins are shown in green with the catalytic residues in red, and α_1PI is in blue and red with the RCL in yellow.

interactions in E·I could give rise to the additional peak. However, the dissociation constant for RTryp−α_1PI encounter complexes is 1.4 μM (*8*); therefore, such complexes should not exist at the picomolar concentrations used in our experiments. To confirm this expectation, we performed spFRET experiments using RTryp containing a mutation of the catalytic Ser to Ala (S195A), which can form E·I but cannot form the acylenzyme intermediate. The spFRET histograms for these complexes show only the 0% peak as expected (Figure 3B, inset). Thus, the extra peak in the spFRET histograms does not arise from the encounter complex.

On the basis of the above results, it is obvious that differences in spectral overlap, donor quantum yields, and/or orientations factors cannot account for the additional peak seen in RTryp versus BTryp covalent complex spFRET histograms, nor does the additional peak arise from the encounter complex. Therefore, the additional peak must arise from covalent complexes in which RTryp is only partially translocated ($E_{part}I^*$) because of interactions with cationic dyes (Figure 4).

Protease Stability Controls the Conformational Distribution. The active site of RTryp is intrinsically more stable than that of BTryp (*27*), which can account for the observation of $E_{part}I^*$ in RTryp but not in BTryp. This hypothesis predicts that destabilizing RTryp will shift the distribution between $E_{part}I^*$ and $E_{full}I^*$. Therefore, we performed spFRET experiments on an RTryp variant containing the Ile16 to Ala mutation. This substitution destabilizes the active site of RTryp by 2.9 kcal/mol (*28*). The spFRET histograms reveal that the mutation reduces the population of $E_{part}I^*$ to 33% of the total with a concomitant increase in $E_{full}I^*$ to 67% (Figure 3D), indicating that stability in and around the protease active site can have a significant effect on the conformational distribution.

DISCUSSION

Conformational Distributions and Protease Stability. RTryp is more stable than BTryp as reflected by its retention of activity at alkaline pH (*27*, *28*) and its unfolding at higher temperatures and guanidine hydrochloride concentrations (data not shown). For the $E_{full}I^*$ conformation, the spFRET histogram peak widths, which reflect the relative mobility of the regions near the dyes, are 17−29% narrower for RTryp than those for BTryp. These consistently narrower RTryp peaks likely reflect RTryp's greater stability and suggest that interactions between α_1PI and BTryp in the $E_{full}I^*$ conformation lead to greater local disruption in the vicinity of residue 113. Differences in the extent of disruption may also result in slightly different positions of the two trypsins relative to α_1PI, as indicated by the differences in the centers of the $E_{full}I^*$ peaks. These spFRET results suggest that protease stability plays an important role in determining the extent of protease structural disruption in protease−serpin covalent complexes.

Translocation and Inactivation. To translocate proteases, serpins must overcome the opposing force of viscous drag (*29*). Raising the solution viscosity or increasing the size of elastase, which also increases the drag, makes α_1PI a worse inhibitor (*29*). Attractive interactions between RTryp and dyes attached to α_1PI augment the opposing drag force, further increasing the energy required for protease translocation, trapping as many as 50% of the complexes in the partially translocated conformation. The partitioning between full and partial translocation could be a thermodynamic effect, where the barriers to trapping and to full translocation are approximately equal. Alternatively, the partitioning could be a kinetic effect, where the dye slows the rate of translocation, increasing the probability that a partially translocated conformation will be trapped.

Models of protease−serpin covalent complex formation suggest that most of the protease structural disruption occurs during the final steps in translocation (*4*). However, the lifetime of $E_{part}I^*$, while not as long as that of $E_{full}I^*$, is 10^5−10^6-fold longer than that of a substrate acylenzyme. Partial translocation or changes in the protease−serpin interactions due to dye−protease interactions must alter the geometry of the active site, perhaps by pulling Ser195 away from the other members of the catalytic triad. These results suggest that significant alterations in the active site geometry could occur early in translocation.

Reducing the energy required to deform the active site increases the energy available to counteract the RTryp−dye attraction. The stability of the salt bridge between the *N*-terminal Ile16 and Asp194, which is adjacent to the catalytic Ser195, is at least partly responsible for the activity of RTryp at high pH, where BTryp loses activity (*27*). This salt bridge is disrupted in both of the covalent complex structures (*5*, *6*), and disruption of the salt bridge should

modulate the conformations of protease−serpin complexes. The Ile16Ala mutation weakens the salt bridge, decreasing RTryp stability by 2.9 kcal/mol, as measured by inhibitor binding (*28*), and reducing the force needed to disrupt the active site. This disruption changes the partitioning between $E_{part}I^*$ and $E_{full}I^*$, either by changing barrier heights or by increasing the speed of translocation due to a more compliant linkage between RTryp and α_1PI. We have not observed $E_{part}I^*$ for BTryp complexes, presumably because of differences in dye−trypsin interactions as well as the lower stability of the BTryp active site. Our ability to trap $E_{part}I^*$ for RTryp as well as our ability to modulate its population demonstrate the importance of protease stability in determining both the number of discrete conformations and the conformational distributions of protease−serpin covalent complexes.

Our single molecule fluorescence studies of protease−serpin covalent complexes also reconcile apparently conflicting observations regarding the structure of protease−serpin complexes, the extent of protease disruption as well as the number of discrete conformations accessible to protease−serpin covalent complexes. These results suggest that the balance between the energy stored in the serpin and the stability of the protease, particularly its active site, are important for the serpin inhibitory mechanism.

ACKNOWLEDGMENT

We thank Qi Wang for expert technical assistance and Professor Daniel Oprian for use of the Fluorolog fluorometer.

SUPPORTING INFORMATION AVAILABLE

Supplementary experimental procedures describing the single molecule anisotropy experiments, detailed schematic of the single molecule fluorescence experimental setup, and the single molecule anisotropy histograms. This material is available free of charge via the Internet at http://pubs.acs.org.

REFERENCES

1. Irving, J. A., Pike, R. N., Lesk, A. M., and Whisstock, J. C. (2000) Phylogeny of the serpin superfamily: Implications of patterns of amino acid conservation for structure and function, *Genome Res. 10*, 1845−1864.
2. Gettins, P. G. W. (2002) Serpin structure, mechanism, and function, *Chem. Rev. 102*, 4751−4803.
3. Ohlsson, K., and Laurell, C. B. (1976) The disappearance of enzyme−inhibitor complexes from the circulation of man, *Clin. Sci. Mol. Med. 51*, 87−92.
4. Gettins, P. G. W. (2002) The F-helix of serpins plays an essential, active role in the proteinase inhibition mechanism, *FEBS Lett. 523*, 2−6.
5. Huntington, J. A., Read, R. J., and Carrell, R. W. (2000) Structure of a serpin-protease complex shows inhibition by deformation, *Nature 407*, 923−926.
6. Dementiev, A., Dobo, J., and Gettins, P. G. W. (2006) Active site distortion is sufficient for proteinase inhibition by serpins: structure of the covalent complex of α_1-proteinase inhibitor with porcine pancreatic elastase, *J. Biol. Chem. 281*, 3452−3457.
7. Peterson, F. C., and Gettins, P. G. W. (2001) Insight into the mechanism of serpin-proteinase inhibition from 2D [^{1}H-^{15}N] NMR studies of the 69 kDa α_1-proteinase inhibitor Pittsburgh-trypsin covalent complex, *Biochemistry 40*, 6284−6292.
8. Mellet, P., Mély, Y., Hedstrom, L., Cahoon, M., Belorgey, D., Srividya, N., Rubin, H., and Bieth, J. G. (2002) Comparative trajectories of active and S195A inactive trypsin upon binding to serpins, *J. Biol. Chem. 277*, 38901−38914.
9. Calugaru, S. V., Swanson, R., and Olson, S. T. (2001) The pH dependence of serpin-proteinase complex dissociation reveals a mechanism of complex stabilization involving inactive and active conformational states of the proteinase which are perturbable by calcium, *J. Biol. Chem. 276*, 32446−32455.
10. Plotnick, M. I., Samakur, M., Wang, Z. M., Liu, X., Rubin, H., Schechter, N. M., and Selwood, T. (2002) Heterogeneity in serpin-protease complexes as demonstrated by differences in the mechanism of complex breakdown, *Biochemistry 41*, 334−342.
11. Hedstrom, L., Szilagyi, L., and Rutter, W. J. (1992) Converting trypsin to chymotrypsin: The role of surface loops, *Science 255*, 1249−1253.
12. Pasternak, A., Liu, X., Lin, T.-Y., and Hedstrom, L. (1998) Activating a zymogen without proteolytic processing: Mutation of Lys15 and Asn194 activates trypsinogen, *Biochemistry 37*, 16201−16210.
13. Peterson, F. C., Gordon, N. C., and Gettins, P. G. W. (2001) High-level bacterial expression and ^{15}N-alanine labeling of bovine trypsin. Application to the study of trypsin−inhibitor complexes and trypsinogen activation by NMR spectroscopy, *Biochemistry 40*, 6275−6283.
14. Huber, R., and Carrell, R. W. (1989) Implications of the three-dimensional structure of α_1-antitrypsin for structure and function of serpins, *Biochemistry 28*, 8951−8966.
15. Kwon, K.-S., Kim, J., Shin, H. S., and Yu, M.-H. (1994) Single amino acid substitutions of α_1-antitrypsin that confer enhancement in thermal stability, *J. Biol. Chem. 269*, 9627−9631.
16. Kwon, K.-S., Lee, S., and Yu, M.-H. (1995) Refolding of α_1-antitrypsin expressed as inclusion bodies in *Escherichia coli*: characterization of aggregation, *Biochim. Biophys. Acta 1247*, 179−184.
17. Griffiths, S. W., and Cooney, C. L. (2002) Development of a peptide mapping procedure to identify and quantify methionine oxidation in recombinant human α1-antitrypsin, *J. Chromatogr., A 942*, 133−143.
18. Chase, T. J., and Shaw, E. (1967) *p*-nitrophenyl-*p′*-guanidinobenzoate HCl: A new active site titrant for trypsin, *Biochem. Biophys. Res. Comm. 29*, 508−514.
19. Rubin, H., Wang, Z. M., Nickbarg, E. B., McLarney, S., Naidoo, N., Schoenberger, O. L., Johnson, J. L., and Cooperman, B. S. (1990) Cloning, expression, purification and biological activity of recombinant native and variant human α_1-antichymotrypsins, *J. Biol. Chem. 265*, 1199−1207.
20. Lakowicz, J. R. (1999) *Principles of Fluorescence Spectroscopy*, 2nd ed., Kluwer Academic Press, New York.
21. Dahan, M., Deniz, A. A., Ha, T., Chemla, D. S., Schultz, P. G., and Weiss, S. (1999) Ratiometric measurement and identification of single diffusing molecules, *Chem. Phys. 247*, 85−106.
22. Schuler, B., Lipman, E. A., and Eaton, W. A. (2002) Probing the free-energy surface of protein folding with single-molecule fluorescence spectroscopy, *Nature 419*, 743−747.
23. Marquart, M., Walter, J., Deisenhofer, J., Bode, W., and Huber, R. (1983) The geometry of the reactive site and of the peptide groups in trypsin, trypsinogen and its complexes with inhibitors. *Acta Crystallogr., Sect. B 39*, 480−490.
24. Guex, N., and Peitsch, M. C. (1997) Swiss-model and the Swiss-pdb viewer: An environment for comparative protein modeling, *Electrophoresis 18*, 2714−2723.
25. Earnest, T., Fauman, E., Craik, C. S., and Stroud, R. (1991) 1.59 Å structure of trypsin at 120 K: Comparison of low temperature and room temperature structures, *Proteins 10*, 171−187.
26. Schuler, B., Lipman, E. A., Steinbach, P. J., Kumke, M., and Eaton, W. A. (2005) Polyproline and the "spectroscopic ruler" revisited with single-molecule fluorescence, *Proc. Natl. Acad. U.S.A. 102*, 2754−2759.
27. Soman, K., Yang, A.-S., Honig, B., and Fletterick, R. (1989) Electrical potentials in trypsin isozymes, *Biochemistry 28*, 9918−9926.
28. Hedstrom, L., Lin, T.-Y., and Fast, W. (1996) Hydrophobic interactions control zymogen activation in the trypsin family of serine proteases, *Biochemistry 35*, 4515−4523.
29. Shin, J.-S., and Yu, M.-H. (2006) Viscous drag as the source of active site perturbation during protease translocation: insights

into how inhibitory proteases are controlled by serpin metastability, *J. Mol. Biol. 359*. 378−389.
30. Dementiev, A., Simonovic, M., Volz, K., and Gettins, P. G. W. (2003) Canonical inhibitor-like interactions explain reactivity of α_1-proteinase inhibitor Pittsburgh and antithrombin with proteinases, *J. Biol. Chem. 278*, 37881−37887.

BI0609568